

AAPM REPORT NO. 217



Radiation Dose from Airport Scanners

Report of AAPM Task Group 217

June 2013

DISCLAIMER: This publication is based on sources and information believed to be reliable, but the AAPM, the authors, and the editors disclaim any warranty or liability based on or relating to the contents of this publication.

The AAPM does not endorse any products, manufacturers, or suppliers. Nothing in this publication should be interpreted as implying such endorsement.

DISCLAIMER: This publication is based on sources and information believed to be reliable, but the AAPM, the authors, and the publisher disclaim any warranty or liability based on or relating to the contents of this publication.

The AAPM does not endorse any products, manufacturers, or suppliers. Nothing in this publication should be interpreted as implying such endorsement.

ISBN: 978-1-936366-24-8

© 2013 by American Association of Physicists in Medicine

All rights reserved.

Published by

American Association of Physicists in Medicine
One Physics Ellipse
College Park, MD 20740-3846

Task Group Members

Christopher H. Cagnon, Ph.D. (Chair)
Department of Radiological Sciences[†]

John M. Boone, Ph.D.
Department of Radiology[‡]

Jerrold T. Bushberg, Ph.D.
Depts. of Radiology and Radiation Oncology[‡]

John J. DeMarco, Ph.D.
Department of Radiation Oncology[†]

Daniel A. Low, Ph.D.
Department of Radiation Oncology[†]

Michael F. McNitt-Gray, Ph.D.
Department of Radiological Sciences[†]

Anthony J. Seibert, Ph.D.
Department of Radiology[‡]

AAPM Staff: Lynne Fairobent

[†]University of California, Los Angeles

[‡]University of California, Davis

Acknowledgements

The members of the task group thank Paul Sunde and Radcal Corporation for their support and expertise.

Contents

1. Introduction.....	2
1.1. What This Report Does and Does Not Address.....	3
2. Background	3
2.1. Scanner Description	3
3. Test Equipment and Methods.....	4
3.1. Detector Calibration	5
3.2. Calibration Results	5
3.3. Measurement Setup and Exposure Uniformity	6
3.4. Exposure Measurements at Reference Point	7
3.5. Dose Calculation Methodology	8
4. Exposure Results and Dose Calculations	9
5. Comparisons to Background and Reference Standards	10
5.1. Reference Standard.....	11
5.2. Skin Dose.....	12
5.3. Operator Exposure	12
5.4. Scanner Failure	13
5.5. Comparison to Other Work	13
6. Discussion.....	15
7. References.....	17

This page intentionally left blank.

Summary

This work represents an independent study by the American Association of Physicists in Medicine (AAPM) of the x-ray backscatter systems used by the Transportation Security Administration (TSA) for screening airport passengers, the *Rapiscan Secure 1000 SP*. Exposure output measurements were made across multiple scanners in both the factory and in real-time use in an airport setting. From these exposure measurements, effective and organ dose calculations were performed for several passenger sizes. The average corrected air kerma measurement across the systems evaluated was 0.046 μGy (for each master or slave unit which together comprise a scanner). For a standard man of 178.6 cm (5'10") tall and 73.2 kg (161.4 pounds), the effective dose from a single-pose, two-sided scan was determined to be 11.1 nSv ($\text{nSv} = 10^{-9}\text{Sv}$) and the skin dose to be 40.4 nGy ($\text{nGy} = 10^{-9}\text{Gy}$). This effective dose is equivalent to 1.8 minutes of background dose received by the average individual in the U.S. in 2006 and is approximately equivalent to 12 seconds of naturally occurring dose during an average flight.

Investigators

All investigators were members of the AAPM and, specifically, members of Task Group 217 as approved by the AAPM Science Council and Imaging Physics Committee. To avoid any appearance of bias, all Task Group members worked on a volunteer basis and received no compensation for this work. Task Group members did receive cooperation from *Rapiscan* personnel in obtaining access to units both in the factory in California and at Los Angeles International (LAX) airport. All measurements, data collection, and analysis were made directly by Task Group members; *Rapiscan* personnel had no oversight or editing authority over this report (but did review the report to ensure that no classified or proprietary information was disclosed).

1. Introduction

In 2007 the Transportation Security Administration (TSA) began deploying imaging devices at airports to scan individual passengers for potential threats.¹ As of this writing, two technologies are currently employed: millimeter wave scanners and backscatter x-ray systems. Both systems use electromagnetic radiation (radio waves and x-rays, respectively) to penetrate through clothing and create a reflected image of the body. This report focuses on the backscatter scanners made by *Rapiscan* (*Rapiscan Systems*, Torrance, CA), specifically the *Secure 1000 SP* scanner used by TSA for screening passengers.

Backscatter x-ray technology uses low-energy, low-output (50 kVp, 5 mA) x-ray to raster scan a pencil beam of photons across the surface of an individual being scanned. The beam penetrates the clothing and sensitive detectors pick up the x-rays that are reflected off the body. An image is created as a function of the backscattered x-ray intensity and known position of the x-ray source. Concealed materials such as liquids, metals, plastics, and ceramics can be detected under a passenger's clothing.² Backscatter x-ray systems were patented in 1993 and prior to airport use have had applications involving security, including prisons, law enforcement, and customs.³

Because the backscatter imaging technology uses x-rays which, while low energy, are still ionizing radiation, there has been considerable public concern over the safety of these devices, especially given the large number of individuals potentially scanned.⁴ The American National Standards Institute (ANSI) in conjunction with the Health Physics Society (HPS) developed standards for such devices which set specific output limits for security screening systems.⁵ Studies have been commissioned by TSA to assess the dose from the *Rapiscan* system and have reported that the dose is both very low and well within ANSI standards for such devices.^{6,7} However, the first of these studies examined a dual-pose model of a different configuration than is currently used by TSA (single-pose, dual-chassis units are currently used) and the second examined an "engineering" model mocked up from component parts by *Rapiscan*. Criticisms have been raised over the reported output and dosimetry values in these studies as to their validity, impartiality (some sections were redacted as the reports were obtained through the Freedom of Information Act), and the appropriateness of the metrics used. A common concern also expressed in articles discussing passenger x-ray backscatter scanners is the need for independent testing.^{8,9}

To address some of these concerns, and in keeping with the mission of the American Association of Physicists in Medicine (AAPM) to educate and disseminate scientific and technical information, the first aim of this report was to utilize the expertise of the medical physics community to make independent, detailed measurements of the *Rapiscan* system output. Our second aim was to make measurements on multiple commercial systems, from both the factory and systems in the field, i.e., scanners in actual use in an airport setting. In contrast to prior studies that extensively characterized a single scanner, our objective in making output measurements on multiple scanners was to help allay concerns that a system may have been specifically selected for evaluation or might otherwise not be representative of scanners in public use. We worked with Rapiscan to gain access to airport scanners without violating security concerns and made our own independent measurements on scanners actively engaged in passenger screening.

A third aim was to provide an estimate of effective dose, as a proxy for assessing risk, calculated from output measurements of the evaluated scanners. As skin dose was expected to be proportionally greater than the effective dose due to the low beam energies used (as compared to traditional medical x-ray imaging), our final aim was to include estimates of skin and other superficial organ dose, as well as detailed calculations of dose deposition in skin tissue for the beam energies used by the scanner. In addition, some context is provided by comparing these estimated dose values to background radiation doses.

1.1 What This Report Does and Does Not Address

It is not the goal of this report to either advocate or discourage use of these systems. Similarly, while observations are offered where appropriate, it is beyond the scope of this report to address the screening efficacy of these systems or any passenger privacy concerns. Both TSA and *Rapiscan* have spent considerable effort to address questions on the latter, and for those wishing to learn more about these subjects, a suggested starting point is the TSA website (www.tsa.gov) under the Innovation and Technology section. In a similar vein, while scatter and leakage measurements were made and are reported, operator exposure was not one of the objectives of this report and, in fact, was found to be too low to be practically measured in a public airport environment with available instrumentation. Those interested can find extensive measurements in TSA-commissioned studies.^{6,7}

2. Background

2.1 Scanner Description

The x-ray backscatter screening system evaluated in this report is the *Rapiscan Systems Secure 1000 SP*. The system is based on the backscatter-imaging device described in U.S. Patent 5181234 (S. Smith, 1991). There are two configurations of the *Secure 1000*. The first is a dual-pose system which uses a single x-ray source and detector array in a single housing and, thus, requires the individual to turn around to scan both front and back. The second (Figure 1) is a single-pose (SP), double-sided system which is comprised of two opposing x-ray source and detector arrays housed in two separate chassis used to scan a subject's front (anterior-posterior projection [AP]) and back (posterior-anterior [PA]) without them having to turn around. Note that the so-called single-pose system requires dual scanners, whereas the dual-pose system uses only a single scanner. The single-pose system is predominantly used by TSA to improve throughput, as the subject does not have to turn around and be re-scanned to achieve full coverage. The single-pose, double-sided scanners are configured in a master-slave configuration where the operator initiates the exposure on the master, and the slave automatically follows to create the AP and PA images (the scans are performed sequentially rather than simultaneously to reduce cross scatter). Unless noted otherwise, all exposure measurements and characterizations in this report are for a single-sided exposure, be it master or slave unit. Dose calculations include exposures from both AP and PA (i.e., both single sided) exposures, and the cumulative dose estimates include the effects from the combined AP and PA scans as performed on passengers.



Figure 1. Rapiscan Secure 1000: single-pose, dual-scan system.

Each scanner is comprised of a small x-ray tube that emits through a small horizontal slit placed in front of the housing. In front of the slit (toward the subject) is a rotating “chopper” wheel with four equally spaced radial slits located around its periphery. The path of the radial slit passing perpendicularly in front of the housing slit results in a pencil beam of x-ray horizontally scanned across the field of view. The entire housing and chopper wheel assembly is vertically translated during the scan to create a raster scanned pattern across the entire field of view. To the sides of the moving x-ray tube and chopper assembly are two vertical arrays of detector screens fluorescing onto photomultiplier tubes. An image is generated based on the intensity of detected backscatter x-rays as a function of pencil beam position. The x-ray tube is operated at a fixed 50 kVp potential with a fixed 5mA tube current, and the entire raster scan for each side takes three seconds. NOTE: for the dual-pose, single scanner, the beam is scanned at a slower rate, and each pose requires approximately six seconds.

3. Test Equipment and Methods

Measuring very low exposures requires radiation detectors appropriate for the task. A large-volume ion chamber provides high sensitivity and has relatively low energy dependence com-

pared to solid-state devices. An 1800 cc chamber (Model 10x5-1800, Radcal, Monrovia, CA) was procured and paired with their 9660 ion chamber digitizer and Accupro control unit. This very large-volume ionization chamber is specifically designed for low-level radiation measurements requiring greater sensitivity and accuracy than traditional survey meters. The published specifications are a minimum dose of 0.2 nGy, a minimum dose rate of 0.05 nGy/s, and air kerma rate dependence of +0%/-5% from 0.243 nGy/s (0.1 mR/h) to 0.485 µGy/s (20 mR/hr).

3.1 Detector Calibration

For the relatively low beam energies used by the *Rapiscan* system, detector calibration—and specifically detector energy response—can result in significant measurement error if not accounted for. Prior to measurement of the *Rapiscan* systems, the electrometer, ion chamber, and test setup were tested in a radiographic room setting to assess reproducibility and linearity at low kVp (50 kVp) and at very low exposure (using large source-to-detector distances to generate exposures in the sub µGy range). The paired chamber and electrometer were also sent to the National Institute of Standards and Technology (NIST) for direct calibration for the specific beam energy used by the *Rapiscan* system. The NIST beam calibration reference code is a function of kVp and beam filtration as expressed by half value layer (HVL) and homogeneity coefficient. To determine the appropriate beam calibration code for the *Rapiscan Secure 1000 SP*, HVL measurements were made both on a laboratory “bench-top” stationary tube assembly in the factory as well as on an operational scanning system in the airport environment. For the former, measurements were made with slot and chopper wheel removed (e.g., no scan motion or cabinet housing) and low scatter geometry was used with a mammography ion chamber. For the latter, the HVL measurements were made on a system in use at the airport using the 1800 cc chamber used to make primary exposure measurements. In the airport environment, it was necessary to account for backscattered photons reaching the sensitive volume during filtration measurements, which was accomplished by using a lead blocker to attenuate the primary beam for a background reading that was subtracted from HVL exposures.

Unless otherwise noted, all measurements were made with the center of the chamber volume positioned at the scanner’s factory measurement reference point: 91.4 cm (36 inches) above the floor and 30.5 cm (12 inches) from the face of the scanner—centered horizontally—with the 1800 cc chamber stem positioned vertically (perpendicular to the central ray). This geometry was also used by NIST for our chamber calibration.

3.2 Calibration Results

An HVL of 0.81 mm aluminum (Al) was determined for the factory bench-top system without chopper assembly and chassis screen. An HVL of 0.93 mm Al was determined for the fully operational system assessed in the airport which is consistent with the slightly greater attenuation afforded by including the chassis housing fascia. Of the available NIST beam qualities, the M50 beam code corresponding to an HVL of 1.04 mm Al was selected as an appropriate match. An energy calibration factor of 1.15 was determined by NIST for our chamber/electrometer for this beam code.

3.3 Measurement Setup and Exposure Uniformity

As noted above, the *Rapiscan Secure 1000 SP* uses a raster-scanning beam which is generated by a horizontally scanning pencil beam and vertically translated x-ray assembly which also pivots throughout its vertical movement. As a result, the x-ray source is not fixed, and the vertical translation/pivot movement results in a relatively constant source-to-subject distance from head to toe. As a consequence, the output measured at the subject location does not follow an inverse square relation with distance from chassis front, as with a conventional x-ray source. The exposure profiles in the vertical and horizontal axis of the *Secure 1000 SP* have been well characterized in previous work,⁶ and measurements were made of the exposure falloff as a function of vertical and horizontal distance relative to *Rapiscan's* exposure calibration reference point. The reference point closely corresponds to the point of maximum exposure in a vertical plane at a given distance from the chassis face with approximately a 10% drop in intensity with a vertical displacement of ± 50 cm from reference and a 34% drop off with a lateral displacement of 20 cm from centerline (note the relatively uniform exposure in the vertical axis). However, for purposes of determining an exposure input value for dose calculation, the exposure is conservatively assumed to be uniform in a coronal plane at the front surface of the scan subject. The exposure falloff with distance from scanner face was assessed with the 1800 cc chamber and is shown in Figure 2.

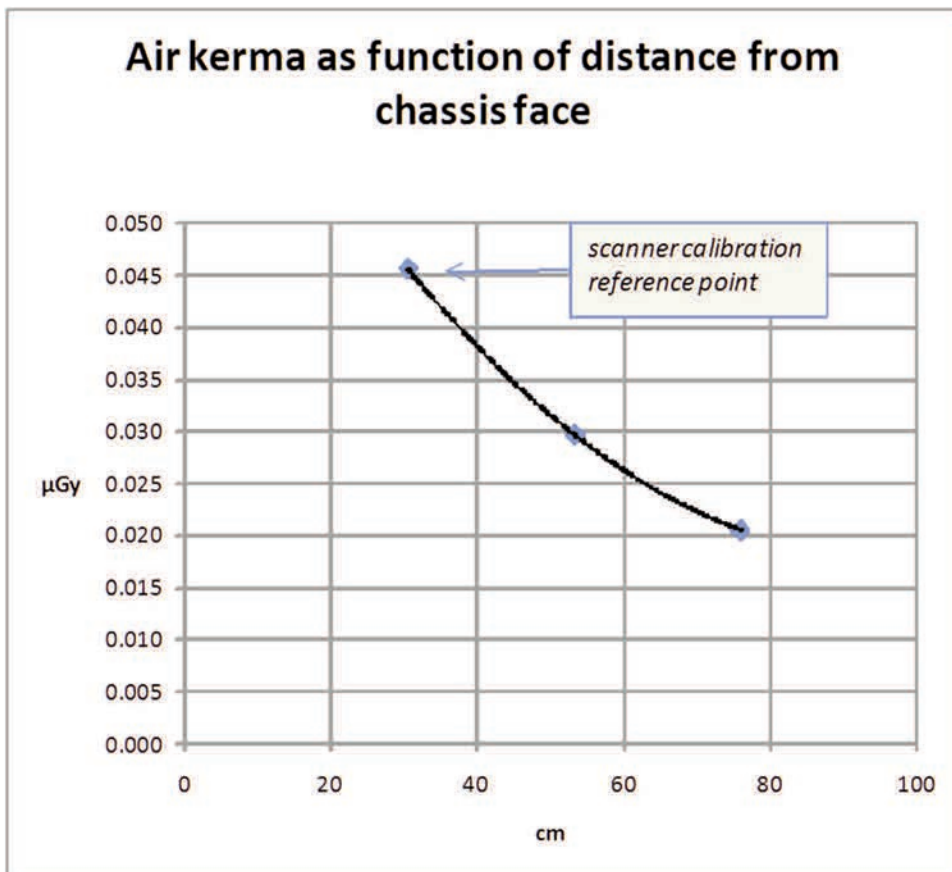


Figure 2. Air kerma as function of distance from chassis.

3.4 Exposure Measurements at Reference Point

Once the *Rapiscan* factory exposure calibration point was validated as the point of maximum exposure in the gantry plane, all scanner output measurements were made at this location: 91.4 cm (3 feet) above the floor and 30.5 cm (1 foot) from the scanner face. As noted above, the master and slave units are identical in functional design and were tested independently (exposure disabled on the opposing unit). An example of the measurement setup and test chamber is shown in Figure 3. For all measurements, the center of the active chamber volume was centered at the reference point, and the full raster scan was executed for either the master or slave unit. The final exposure reading was taken as the average of a minimum of 10 independent scans.

In all a total of nine separate master and slave subunits were assessed for exposure output, three in the factory and six at the Los Angeles International Airport (i.e., three complete systems at two different terminals). Two of the airport scanners were in active use at the time of measurement, and passenger traffic was diverted temporarily to an adjoining lane while measurements were made.



Figure 3. Measurement setup.

Due to the large size of the chamber, there was expected to be some experimental measurement setup variability. To get an estimate for the reproducibility of our measurements, separate readings were made where the test setup was moved out of, and re-located back to, the scanner reference point, resulting in a maximum difference in measured air kerma of 3.7%.

3.5 Dose Calculation Methodology

To make a determination of the effective and organ dose from measured exposure, the dose calculation package PCXMC 2.0 (STUK–Radiation and Nuclear Authority, Helsinki, Finland) was used.^{10,11} PCXMC is a Monte Carlo simulation program that uses the anthropomorphic mathematical models of Cristy and Eckerman^{12,13} to calculate organ and effective dose for a range of six different patient ages from newborn to adult, and it uses tissue weighting factors for effective dose estimation recommended by the International Commission on Radiological Protection (ICRP) Report 103.¹⁴ The software also allows for the phantom size to be adjusted to any arbitrary height and weight, and sample dose calculations were performed for the *Rapiscan 1000* for a range of patient sizes. Note that Cerra also used a prior version of this dose calculation software in 2006 for work done on the airport scanner by the U.S. Food and Drug Administration's (FDA) Center for Devices and Radiologic Health (CDRH).⁶

Dose estimation requires information about beam spectra and beam geometry. The x-ray spectra for photon transport is determined by user-defined input variables for tube potential (kVp), x-ray target angle, and total beam filtration. The PCXMC beam geometry allows for arbitrarily defined rectangular field sizes and projection angles. Specific details for input variables and dose calculation assumptions are as follows. The beam spectrum was characterized using a tube potential of 50 kVp and an anode angle of 20 degrees.¹⁵ The measured HVL of an x-ray tube is a function of total filtration and kVp. For our measured HVL of 0.93 mm Al and tube potential of 50 kVp, the total filtration was determined to be 1.0 mm Al.¹⁶

Doses for AP and PA projections were separately calculated, reflecting the master (AP) and slave (PA) configuration of the *Secure 1000 SP* used by TSA. PCXMC either assumes a point source for a diverging x-ray beam or allows for a parallel beam projected x-ray source with unidirectional x-ray photons useful for emulating point scanning x-ray beams. For our dose estimates, we used the parallel x-ray beam for transport through the simulation phantom, which we believe is a better (and more conservative) approximation for the *Secure 1000 SP* that vertically translates the x-ray source during the scan. However, while a parallel beam was used for photon transport through the phantom, a distance-corrected adjustment of the x-ray exposure input value to PCXMC was made based on the estimated location of the input surface of the phantom to reflect where the passenger would likely be positioned for screening between the master/slave chassis and accounting for the measured exposure falloff from the face of the scanner chassis shown in Figure 2. Thus for the PCXMC standard man phantom (height 178.6 cm, mass 73.2 kg) the AP dimension is 20 cm for the torso. Locating the simulation phantom where the scan subject is expected to stand—centered between master and slave unit of the *Secure 1000 SP* (screen face to screen face is 106.68 cm or 42 inches)—places the input surface of the phantom at 43.3 cm from the chassis screen (Figure 4). A polynomial regression analysis of the exposure drop-off with distance (shown in Figure 2) indicates that the distance-corrected exposure (free in air) at 43.3 cm to be 77% of the measurement at reference point 30.5 cm (12 inches) from

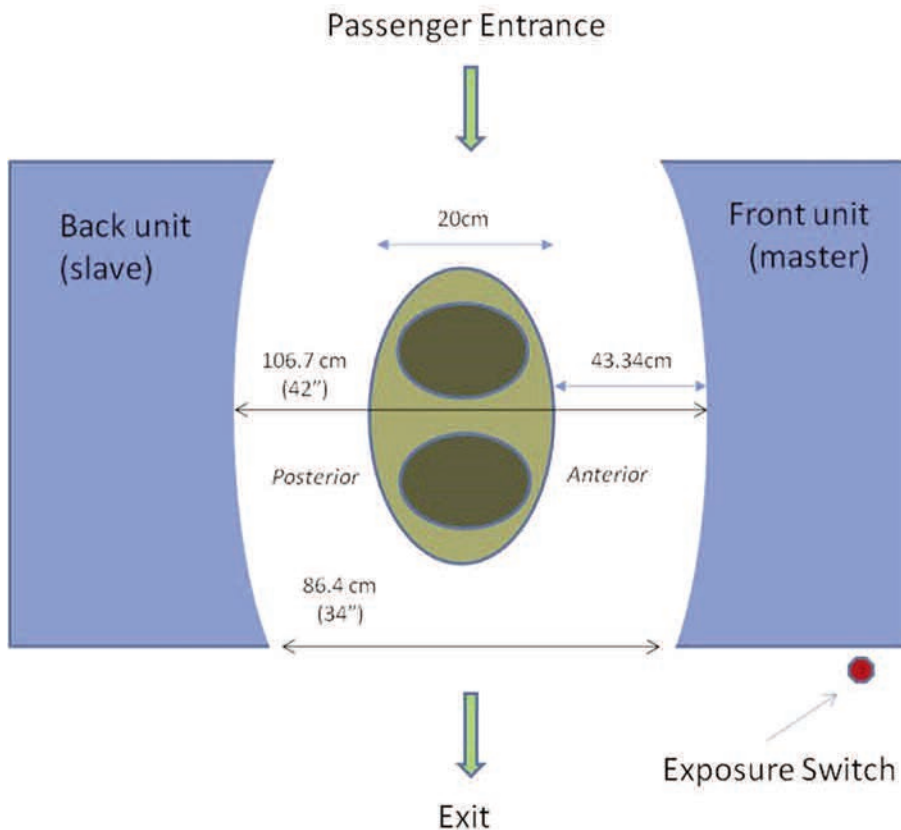


Figure 4. Geometry of Rapiscan Secure 1000 showing placement of anthropomorphic dose simulation phantom (not to scale).

chassis screen face. Entrance exposure values were similarly adjusted for the other phantom sizes used in the calculations. For all PCXMC Monte Carlo simulations 1×10^6 photons were transported, sufficient to provide less than an estimated 2.5% error in effective dose for all simulations. For all simulations, the dimensions of the x-ray beam were specified to irradiate the entire phantom from head to toe.

4. Exposure Results and Dose Calculations

The energy-corrected air kerma measurements at reference point averaged for all tested units was 0.046 μGy with a standard deviation of 0.003 μGy and a range of 0.04 μGy to 0.052 μGy . This average exposure value, corrected for distance to the phantom entrance plane, was used for all PCXMC calculations. The default adult Cristy phantom representing a “standard man” has a height of 178.6 cm (5 feet, 10 inches) and a weight of 73.2 kg (161.4 pounds). As this underestimates the average size of the adult population in the United States, the average heights and weights for an adult U.S. man and woman over age 20 were obtained from the 2003–2006 National Health Statistics Report produced by the Centers for Disease Control and Prevention (CDC) and also used as input data for dose estimation.¹⁷ To round out the comparison, dose estimates were also made for a 10 year old as defined by the PCXMC software and for a U.S. adult

in the 90th percentile in size. All phantom sizes and estimates of their “effective” dose in nanoSieverts (1 nSv = 10⁻⁹ Sv), as well as separate organ doses for skin, breast, and thyroid in nanoGrays (nGy) are shown in Table 1. ICRP defines effective dose for reference phantom standard man; doses for other subject sizes are calculated in the same fashion for comparison purposes. Note that doses for the AP (master) and PA (slave) projection are listed separately, along with the subsequent cumulative screening (two scans) doses. Note also that larger-size subjects receive somewhat smaller doses, and smaller subjects receive larger doses, even when accounting for their respectively smaller and greater distances from the scanner face due to their different thicknesses. This is not due to variation in machine exposure, but is a result of the different absorption patterns due to differences in tissue mass of the scanned subjects (absorbed dose is energy absorbed per unit mass). A similar phenomenon is experienced in medical x-ray procedures where smaller patients receive more dose for a given machine output as a result of their smaller size/mass.

5. Comparisons to Background and Reference Standards

When attempting to explain radiation exposure to the lay public, a commonly used comparison is background radiation, which is naturally occurring in our environment from inhalation (radon), space (cosmic), terrestrial (soil and structures), and internal (our own bodies) sources. While the magnitude of background radiation can vary considerably depending on where one lives, the National Council on Radiation Protection and Measurements (NCRP) has compiled an

Table 1. “Effective” and organ doses for select subject sizes.
1 nSv = 1 x 10⁻⁹ Sv (one billionth of a Sievert).

Monte Carlo phantom	height (cm)	height (ft, in)	mass (kg)	mass (lb)	projection	Effective dose (ICRP 103) in nSv	skin dose (nGy)	breast dose (nGy)	thyroid dose (nGy)
“Standard” man	178.6	5' 10"	73.2	161.4	AP	8.0	20.4	19.1	20.0
					PA	3.0	20.0	0.8	1.0
					COMBINED	11.1	40.4	19.9	21.0
10 year old	139.8	4'7"	32.4	71.4	AP	11.1	21.3	31.9	21.0
					PA	3.7	21.1	0.9	1.4
					COMBINED	14.8	42.4	32.8	22.4
CDC average U.S. adult	169.2	5'7"	81.5	179.7	AP	7.6	20.8	18.6	18.9
					PA	2.8	20.3	0.6	0.9
					COMBINED	10.4	41.0	19.2	19.9
CDC 90th centile adult	178.4	5'10"	106.6	235.1	AP	7.0	20.7	18.2	17.4
					PA	2.4	20.2	0.5	0.7
					COMBINED	9.38	40.9	18.7	18.2

average effective dose per individual in the U.S. for 2006 which for background only (omitting medical, occupational, and industry/consumer sources) is estimated at 3.11 mSv (mSv = 10^{-3} Sv).¹⁸ A comparison can be made of the effective dose from a single screening from a single-pose, dual-source *Rapiscan Secure 1000 SP* scanner to a standard man of 73.2 kg and the amount of background radiation that individual would normally receive in a given period of time. An effective dose of 11.1 nSv to a standard man from a single-pose x-ray backscatter scan thus equates to 1.9 minutes of normal average background radiation exposure. The effective dose received by an adult closer in size to the average size U.S. citizen (81.5 kg average for men and women) is 10.4 nSv, which equates to 1.8 minutes of background exposure.

The radiation dose at altitudes traveled by commercial airplanes is considerably greater than at sea level due to decreased atmospheric attenuation of natural galactic cosmic and solar cosmic radiation.¹⁹ The amount of dose varies considerably with altitude, latitude, and solar activity. With an average dose rate for domestic flights of 3.30 μ Sv (μ Sv = 10^{-6} Sv) per air hour (with a standard deviation of 1.81 μ Sv per air hour) and an average air time of 2.84 hours, the average dose for domestic flights is 9.4 μ Sv.¹⁸ Thus the dose to a standard man from the *Rapiscan Secure 1000 SP* is equivalent to 12 seconds of naturally occurring dose during an average flight.

5.1 Reference Standard

ANSI and the HPS have issued a standard (ANSI/HPS N43.17 2009) that “applies to the manufacture and operation of security screening systems that are intended to expose humans to primary beam x-rays, gamma radiation, or both.” Our measurements indicate that the effective dose from a single screening exam is well below the screening limit of 0.25 μ Sv per screening for a general use, full-body scanner.⁵ The standard also states that the effective dose (computational adult model) shall not exceed 250 μ Sv over a 12-month period. For our estimated effective dose of 11.1 nSv to a standard man from a single screening, an individual would need to go through more than 22,500 screenings in a year to reach this limit.

In 2003 the NCRP at the request of the FDA issued a commentary (No. 16) on *Screening of Humans for Security Purposes Using Ionizing Radiation Scanning Systems*. In this commentary, the NCRP concludes that for general-use systems, the effective dose from each screening scan should be less than 0.1 μ Sv (nine times higher than the effective dose determined in this report for a standard man). The commentary also refers to a prior 1993 recommendation that “no single source or set of sources under one control should result in an individual being exposed to more than 0.25 mSv annually” (used in the ANSI/HPS standard). The commentary extends the 0.25 mSv annual effective dose limit recommendation to members of the general public for security screening procedures with x-ray scanning devices. NCRP Commentary No. 16 also reviews the concept of negligible individual dose (NID) described in 1993. The NID is described as “an effective dose corresponding to the level of average annual excess risk of fatal health effects attributable to radiation exposure below which effort to further reduce the exposure to an individual is not warranted.” For comparison, the NID was set at an annual effective dose of 10 μ Sv per source or practice (approximately 900 times higher than the effective dose from a single screening scan determined in this report).

5.2 Skin Dose

While effective dose is a calculated quantity that considers dose received by all organs and tissues and the radiation sensitivity of those tissues, most of the dose from these scanners will be absorbed by the skin. This is due to the low penetrating ability of the relatively low-energy x-ray beam which generates proportionately higher dose in skin and lower dose in radiosensitive internal organs. This section looks in more detail at radiation dose absorbed by the skin.

As a means of providing additional information to interested parties, we have also included Monte Carlo simulations evaluating the dose falloff as a function of depth in a simple skin model. The MCNPX Monte Carlo code (Los Alamos National Laboratory) was used to model the bremsstrahlung spectrum from the NIST-equivalent M50 x-ray beam based on a 50 keV monoenergetic electron source incident on a tungsten target. The spectral simulation included inherent filtration of 1 mm Be and added filtration of 1.07 mm Al. Post processing of the simulated spectra produced an HVL and homogeneity coefficient equal to 0.95 mm of Al and 0.70 respectively, in reasonable agreement compared to the NIST stated values of 1.04 mm Al and 0.68 homogeneity coefficient. The skin tissue is modeled as a simple planar geometry, assuming an epidermal layer equal to 1 mm and a dermal layer equal to 3 mm (skin thickness varies with location on body). The elemental composition of skin is taken from ICRU 44 with a density of 1.1 g/cm³. The skin layers are backed by a 20 cm section of ICRU 44 soft tissue. As described previously, the *Rapiscan Secure 1000 SP* x-ray source movement is basically a raster scan pattern across the surface of the backscatter object. For purposes of depth dose analysis, a planar 10 x 10 cm source was modeled incident on the tissue phantom to simulate the broad beam geometry experienced by the skin, and absorbed dose was scored in 1 mm increments.

Figure 5 illustrates the dose falloff for the M50 beam model as a function of depth in the skin/tissue phantom with the dose normalized to one at the surface of the skin model (0.5 mm depth). The depth dose value falls to approximately 80% of the maximum surface value at a depth of 4 mm, corresponding to the distal border of the dermis layer and the dermis-tissue interface. These results are consistent with the Monte Carlo analysis of Hoppe and Schmidt who used voxelized phantoms based on a male and female adult and a male and female child and the GEANT4 toolkit to evaluate organ dose as a function of frontal and rear scans from the x-ray backscatter system.²⁰

5.3 Operator Exposure

While operator exposure was not a primary goal of this report, and scatter and leakage analysis has been performed by others,^{6,7} our group took advantage of having access to the *Rapiscan Secure 1000 SP* in the airport setting to make some rudimentary measurements of scatter and leakage exposure. To simulate a scattering medium, an anthropomorphic torso phantom was placed between the master and slave units (Figure 6) and measurements were made around the periphery of the master and slave units with both our Radcal 1800 cc chamber and a Fluke Biomedical 451P pressurized survey meter (0 to 500 μ R/hr).²¹ Both meters were used to integrate the scatter exposure of 10 consecutive scans from first the master and then the slave unit. Measurements were made at a plane parallel to the sides of the *Secure 1000 SP* chassis in the middle of the gantry opening and immediately at the sides of the master and slave units'

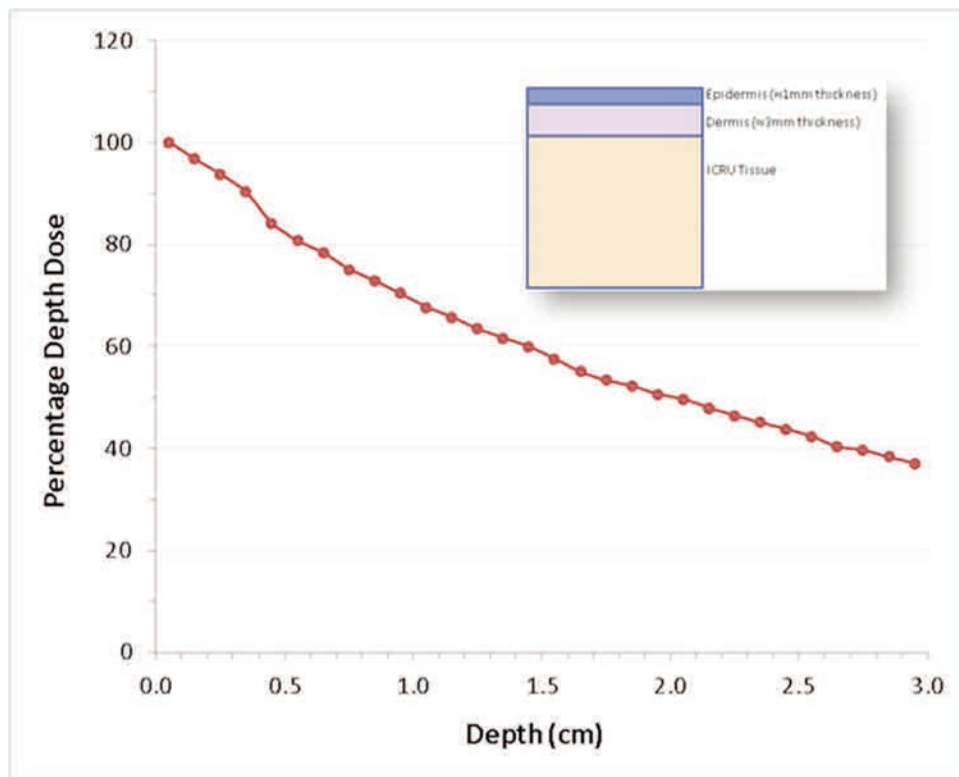


Figure 5. Monte Carlo-calculated depth dose distribution for 50 kVp x-rays incident on a simplified skin model.

scanner chassis (and adjacent to the exposure release switch). In all cases, exposures were below the detection limits of our equipment.

5.4 Scanner Failure

A commonly voiced concern regarding airport scanners is what could happen to an individual's dose if the scanner malfunctions. The ANSI/HPS N43.17 2009 standard includes requirements for controls and safety interlocks for body screening systems, and specifics for the scanner can be found at TSA and *Rapiscan* websites. It was beyond the scope of this report to perform an analysis of the fail-safe mechanisms built into the *Secure 1000 SP*, but we offer two observations: 1) The x-ray tube output is fixed, and by its nature is extremely unlikely to increase in the event of a catastrophic failure, 2) Should it be possible for the mechanisms controlling the raster scanning pattern of the x-ray pencil beam to fail and the beam to become "stuck" while still producing x-ray, the system will no longer be able to produce an image, and such a failure would be immediately evident to the operators.

5.5 Comparison to Other Work

The calculated effective dose from this study is lower than, but generally agrees with, two prior studies contracted by TSA. The first of these studies was performed in 2006 by the FDA CDRH but was restricted to an evaluation of a single older *Secure 1000* model that performed a



Figure 6. Scatter-leakage measurement setup (Fluke 451p above and Radcal 1800 cc chamber below).

single-sided scan with a slower sweep speed.⁶ For comparison, the corrected exposure for the CDRH study was 0.084 μGy (9.6 μR) with a calculated effective dose of 24 nSv to a standard man from a single sided frontal scan. Note that the effective dose calculation for the CDRH study used the 1991 ICRP Report 60 tissue/organ weighting factors, which have since been updated in ICRP Report 103 in 2007. The latter weighting factors were used for our calculations and result in a slightly smaller effective dose than would be determined using the former.

The second of these studies was performed by the Johns Hopkins Applied Physics Laboratory (JHAPL) in 2009 on a scanner configuration similar to those evaluated in this study, but which was an engineering unit built from components in the *Rapiscan* inventory.⁷ The Hopkins study used different exposure-correction factors and chamber orientation, and it came up with a slightly lower (~14%) corrected exposure at reference point (30 cm from panel) of 0.04 μGy (4.6 μR). Their effective dose calculation was based on dose conversion coefficients for determining dose from air kerma and HVL measurements derived from the ANSI/HPS N43.17-2009 report (which also encompasses the performance standards TSA directed JHAPL to determine compliance with). For comparison, the total effective dose determined by JHAPL for a single-pose, two-sided scan screening was 14.8 nSv (1.48 μrem).

The Hoppe and Schmidt article used the exposure values from the JHAPL study and four specific voxelized models of adults and children to determine organ and effective dose based upon their own Monte Carlo model of the *Rapiscan* x-ray system.²⁰ Hoppe and Schmidt deter-

mined the effective dose to a male adult to be 50 nSv and 30 nSv at 30 cm and 75 cm respectively from the x-ray source. For the adult female, the corresponding values were 60 nSv and 30 nSv. For comparison, our study assumes the subject is centered between the two x-ray sources, producing a total effective dose from a single-pose, two-sided scan to be 11.1 nSv for a standard man. The relatively large difference between the total effective dose estimates for Hoppe-Schmidt and the other studies are presumably due to assumptions related to the Monte Carlo models used (PCXMC vs. GEANT4), how the x-ray source itself was modeled, and how the passenger's body was modeled (standard MIRD computational phantoms vs. voxelized patient models).

6. Discussion

The medical physicist or health physicist is often asked about dose and risk from airport scanners, and the subject continues to be of concern to the public at large. The work presented here represents an independent assessment of the exposures and subsequent determined dose from the *Rapiscan Secure 1000 SP* x-ray backscatter scanner used for security screening of airport passengers. While the scanners evaluated in this study represent a limited sample of the total installation base, they also represent the first independent assessment of multiple scanners, including those in active airport use and we have no evidence that other units in use would perform differently.

Effective and organ doses determined from the exposures generated by these scanners were calculated using Monte Carlo simulations using mathematical models of human anatomy. Certain conservative assumptions are built into these models. We assume an input exposure that is uniform in a coronal plane equal to that of the highest exposure at reference distance when, in fact, the exposure falls off somewhat to the sides and the superior and inferior aspects of the plane. The passenger's own clothes will also attenuate the x-ray to some extent. The total dose and dose distribution to an individual may vary depending on one's shape, size, and distribution of radiosensitive tissues. However, these uncertainties in dose estimates are assumed to be small relative to the large uncertainties and assumptions in assessing biological risk from these small doses.

As stated in the European Commission's Scientific Committee on Emerging and Newly Identified Health Risks (SCENIHR): *Health Effects of Security Scanners for Passenger Screening (based on x-ray technology)* in 2012: short-term deterministic effects of tissue damage cannot occur at doses delivered by security scanners. Long-term stochastic effects such as cancer risk are assumed to be directly proportional to received dose with no safe threshold. The cancer risk cannot be estimated with any precision, but is likely to be so low as to be indistinguishable from other background risks. The risk to the individual is thought to be close to zero for a scanned individual, but "at the population level the possible effect cannot be ignored in the assessment of acceptability of the introduction of the security scanners using x-rays for passenger screening."²² For perspective, we think it important that this potential increase in risk to the population be considered in light of the presumed increase in risk originating from the much greater radiation exposure from the flight itself.

Parties interested in a more in-depth discussion of risk from airport scans can refer to an article published last year (2011) in the Archives of Internal Medicine by Mehta and Smith-Bindman. While the airport scanner effective and organ doses used in their risk calculations are assumed values (e.g., 0.1 μSv) that are considerably higher than the doses reported here, the article discusses cancer risks in the context of normally occurring cancers and concludes that the risks are “truly trivial” even with their higher values.⁹

References

1. Transportation Safety Administration. 16 June 2011. www.tsa.gov.
2. Rapiscan Systems. Hawthorne, CA. 10 June 2011. <http://www.rapiscansystems.com/en/products/ps>.
3. Patent bibliographic data: US5181234A, 1993-01-19, Espacenet, 12 Jun 2012. http://worldwide.espacenet.com/publicationDetails/biblio?CC=US&NR=5181234&KC=&FT=E&locale=en_EP.
4. Brenner, D.J. (2011). "Are x-ray backscatter scanners safe for airport passenger screening? For most individuals, probably yes, but a billion scans per year raises long-term public health concerns." *Radiology* 259:6–10.
5. American National Standard – Radiation Safety for Personnel Security Screening Systems Using X-ray or Gamma Radiation. Approved by American National Standards Institute, Inc. August 2009. Health Physics Society, 2009.
6. Cerra, F. "Assessment of the Rapiscan Secure 1000 Body Scanner for Conformance with Radiological Safety Standards." Department of Health and Human Services, Food and Drug Administration, Center for Devices and Radiologic Health. 21 July 2006.
7. Johns Hopkins University. Applied Physics Laboratory. "Radiation Safety Engineering Assessment Report for the Rapiscan Secure 1000 in Single Pose Configuration." October 2009.
8. Sedat, J., et al. Letter to Department of Health and Human Services. April 2011.
9. Mehta, P., R. Smith-Bindman. "Airport Full Body Screening: What is the Risk." *Arch Intern Med.* Published online March 28, 2011. doi:10.1001/archinternmed.2011.105.
10. Tapiovaara, M., T. Siiskonen. STUK-A231/NOVEMBER 2008. Helsinki: Finnish Centre For Radiation and Nuclear Safety, 1997.
11. Servomaa, A., M. Tapiovaara. (1998). "Organ Dose Calculation in Medical X Ray Examinations by the Program PCXMC." *Radiat Prot Dosimetry* 80:213–219.
12. Cristy, M. "Mathematical Phantoms Representing Children of Different Ages for use in Estimates of Internal Dose." NUREG/CR-1159, ORNL/NUREG/TM-367. Oak Ridge National Laboratory, 1980.
13. Cristy, M., K.F. Eckerman. "Specific absorbed fractions of energy at various ages from internal sources. I. Methods." Report ORNL/TM-8381/V1. Oak Ridge National Laboratory, 1987.
14. Annals of the ICRP. Publication 103. The 2007 Recommendations of the International Commission on Radiological Protection.
15. Personal communication. Andy Kotowski, Chief Technology Officer, Rapiscan Systems, Hawthorne, CA. 06-Jun-2012.
16. Conference of Radiation Control Program Directors (CRCPD) Q.A. Collectible – Beam Quality: Total Filtration and Half Value Layer. October 2001.
17. McDowell, M., et al. "Anthropomorphic Reference Data for Children and Adults: United States, 2003-2006." National Health Statistics Reports. Number 10. 22 October 2008.
18. National Council of Radiation Protection and Measurements. *Report 160: Ionizing Radiation Exposure of the Population of the United States*. March 2009.
19. National Oceanic and Atmospheric Administration (NOAA). Space Weather Prediction Center: Notes on the Natural Radiation Hazard at Aircraft Altitudes. Updated 2007.
20. Hoppe, M.E., T.G. Schmidt. (2012). "Estimation of organ and effective dose due to Compton backscatter security scans." *Med Phys* 39:3396–3403.

21. Fluke Biomedical. 451p survey meter specifications. 06 June 2012. www.flukebiomedical.com.
22. European Commission's Scientific Committee on Emerging and Newly Identified Health Risks (SCENIHR): Health Effects of Security Scanners for Passenger Screening (based on X-ray technology). April 2012.